Analysis of Microresonator-Based Logic Gate for High-Speed Optical Computing in Integrated Photonics

Chenghao Feng, Zhoufeng Ying, Zheng Zhao, Rohan Mital, David Z. Pan, *Fellow, IEEE*, and Ray T. Chen, *Fellow, IEEE*

***Abstract*—Microresonator modulators are commonly used as electrical-optic (EO) logic gates in computing systems on silicon photonics platform. In this article, we provide a compact analytical model to describe the switching properties of a linearly cascaded microresonator modulator array. The analytical model is verified by simulations on commercial software. Switching properties of microresonators under different modulation conditions are investigated. Furthermore, computing modules where microresonator modulators are cascaded in series are also discussed, where the model of microresonators is provided by AIM Photonics Process Design Kit (PDK). Factors that deteriorate the logic outputs are analyzed and methods to improve the accuracy of logic outputs are proposed and demonstrated with 8 microresonator modulators.**

***Index Terms*—Microresonator, logic gate, analytical model, switching property, modulator array.**

I. Introduction

USING photonic integrated circuits (PIC) to do computing has gained extensive attention recently [1]–[6]. The power consumption and transmission bandwidth of silicon electronics have been approaching the inevitable limits with difficulties of scaling down transistors and on-chip metal interconnects. A new generation of technology to continue Moore's law is demanded [7], [8]. Silicon photonics is believed to be one promising alternative to convey and process information, which is fast and compatible with complementary metal-oxide-semiconductor (CMOS) fabrication process. One can integrate electronic components and optical components on a single chip, enable inner-chip communications between electronics and photonics, and realize some complex computing modules [9], [10].

Manuscript received May 8, 2019; revised September 10, 2019 and November 18, 2019; accepted December 12, 2019. Date of publication October 17, 2020; date of current version January 16, 2020. This work was supported by the Air Force Office of Scientific Research (Multidisciplinary University Research Initiative program) under Grant FA 9550-17-1-0071. *(Corresponding author: Ray T. Chen.)*

The authors are with the Microelectronics Research Center, Department of Electrical and Computer Engineering, University of Texas at Austin, Austin, TX 78758 USA (e-mail: fengchenghao1996@utexas.edu; zfying@utexas.edu; zzhao.ee@gmail.com; rmital@utexas.edu; dpan@ece.utexas.edu; chenrt@austin.utexas.edu).

Color versions of one or more of the figures in this article are available online at http://ieeexplore.ieee.org.

Digital Object Identifier 10.1109/JSTQE.2019.2960949

Optical microresonator modulators, especially microrings or microdisks modulators are widely used in high-speed optical computing because of its small footprint and low power consumption [11]–[15]. In digital computing, rings/disks have been adopted as electrical-optic (EO) logic gates in different digital subsystems like XOR gates, full adders, comparators, encoders/decoders, and parity checkers [16]–[25]. For example, architectures composed of microresonator modulator arrays are proposed provided with experimental results of 2 cascaded modulators at 500 Mb/s [2], [25]. Such microresonator-based circuits claim to have a high computing speed up to tens or hundreds of Gb/s thanks to numerous experimental demonstrations of high-speed microresonator modulators [12], [14], [15]. However, the dynamic behaviors of cascaded rings/disks modulator arrays in these computing systems are essential to the performance of the whole system and will determine the feasibility of high-speed computing, which is not discussed in these works and will be investigated thoroughly hereinafter.

There have been numerous works investigating the dynamics of microresonator modulators modulated by sinusoidal waves [26]–[31]. For example, some works [26], [28] use time-dependent transfer matrix to obtain the transmission of rings/disks using Neuman series. Other works [27], [29] obtain the dynamic transmission via temporal coupled-mode theory (TCMT). However, most of them focus on the dynamics of microresonators under periodic modulation and small signal model approximation are used. In optical computing, modulators are driven by aperiodic large digital signals [20]. In addition, the mathematical expressions of these models are also quite complicated, which may prevent us from understanding the switching properties of microresonator modulator array easily. Therefore, a compact model suitable to analyze the performance of microresonator modulators as EO logic gates should be proposed.

Furthermore, multiple logic signals will be operated on cascaded microresonator modulators simultaneously in a computing subsystem. To the best of our knowledge, the dynamics of cascaded microresonator modulators have not been discussed before in the context of digital optical computing. Because microresonator is a resonant structure, we should be cautious when a linear array of microresonators are cascaded.

1077-260X © 2019 IEEE. Personal use is permitted, but republication/redistribution requires IEEE permission.
See https://www.ieee.org/publications_standards/publications/rights/index.html for more information.

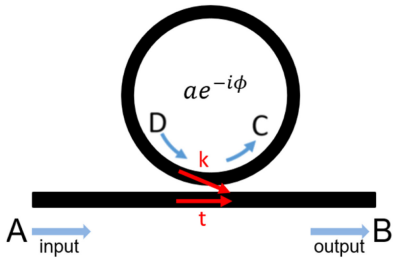

Fig. 1. Schematic of a Ring Resonator.

In this paper, we first solve the exact analytical dynamics of a ring resonator when it functions as EO logic gates in optical computing. Our deduction is based on the transfer matrix model and multiple-round loop approach. The ring is driven by NRZ signals. The step response of rings is analyzed. A compact formula is developed to describe the switching properties of rings under different modulation conditions. Our model is then verified via commercial simulation software. Then we focus on switching properties of a single microring resonator. Furthermore, computing systems where multiple microresonator modulators are cascaded along with the factors that deteriorate the logic output are discussed. Methods to increase accuracy and improve the shape of output waveform are also proposed as last.

II. Theory

In this section, we will describe the switching dynamics of waveguide-coupled microresonator modulator and take microring modulator as an example [32]. The schematic of a ring resonator is illustrated in Fig. 1. The field relationships are [26]:

$$\begin{aligned} B(t) &= r(t)A(t) + ik(t)D(t) \\ D(t) &= C(t-\tau)a(t)e^{-i\phi(t)} \\ C(t) &= r(t)D(t) + ik(t)A(t) \end{aligned} \tag{1}$$

where *A(t)* is the input optical field at time *t*, τ is the resonator round trip delay time. We suppose $A(t) = A$, a constant. At time *t*, *B(t)* is the output optical field, *a(t)* is the attenuation after each round-trip, and *r(t)*, *k(t)* are the resonator transmission and coupling coefficient for the coupler.

To obtain the output field *B(t)*, Eq. (1) needs to be simplified. It can be inferred from Eq. (1) that *D(t)* can be expressed by *B(t)* and *A(t)*, while $C(t-\tau)$ can be expressed by *D(t)*, After eliminating fields in ring *C(t)* and *D(t)*, one can have:

$$\begin{aligned} B(t) = r(t)A(t) + \frac{k(t)}{k(t-\tau)} \\ \times (r(t-\tau)B(t-\tau) - A(t-\tau))a(t)e^{-i\phi(t)} \end{aligned} \tag{2}$$

Here we consider the modulation of the refractive index, where $\phi(t)$ is altered while *a, r* are constant. Using the multiple-round loop approach [30], we can eliminate *B* on the right side of Eq. (2) and expand *B*(t) in the series of $A(t-k\tau)$. The expression would be [28]:

$$B(t) = rA(t) - \sum_{k=1}^{\infty}\left(\frac{1}{r} - r\right)(ra)^k e^{-i\sum_{m=0}^{k-1}\phi(t-m\tau)}A(t-k\tau) \tag{3}$$

where the first term *rA*(t) is the instantaneous response of the resonator, while the second term refers to response contributed by the light coupled to the ring at time $t-k\tau$.

We assume the electrical charging/discharging time of each modulator is negligible. In optical computing, rings are modulated by digital NRZ signals. When refractive indexes are modulated, phases of rings are then switched between two values to represent logic 0 s and logic 1 s, respectively. Therefore, the phase change when the ring is switched from ϕ_0 to ϕ_1 can be treated as a step function with time *t*:

$$\phi(t) = \begin{cases} \phi_0 & t \le 0 \\ \phi_1 & t > 0 \end{cases} \tag{4}$$

When, $t \le 0$ the microring is in steady state. *B(t)* can be calculated directly using the transfer matrix method. We are interested in *B*(*t*) when $t > 0$.

Here we divide light coupled out from the ring into two categories when $t = N\tau$ (*N* is a positive integer): light coupled into the ring at $t \le 0 (k \ge N)$ and light coupled into the ring at $t > 0 (k < N)$. Substitute Eq. (4) into Eq. (3), one can obtain:

$$\begin{aligned} B(N\tau) = rA - \left(\frac{1}{r} - r\right) \\ \times \left(\sum_{k=1}^{N}(ra)^k e^{-ik\phi_1} + \sum_{k=N+1}^{\infty}(ra)^k e^{-i(N\phi_1 + (k-N)\phi_0)}\right)A \end{aligned} \tag{5}$$

Equivalently, we can rewrite Eq. (5) as:

$$\begin{aligned} B(N\tau) = rA - \left(\frac{1}{r} - r\right)\left(\sum_{k=1}^{\infty}(ra)^k e^{-ik\phi_1}\right. \\ \left. + (ra)^N e^{-iN\phi_1}\sum_{k=1}^{\infty}\left((ra)^k e^{-ik\phi_0} - (ra)^k e^{-ik\phi_1}\right)\right)A \end{aligned} \tag{6}$$

Eq. (6) can be analytically solved by calculating geometric series. The complete solution of transmission $T(t = N\tau)$ can then be written as:

$$\begin{aligned} T(N\tau) = \frac{B(N\tau)}{A} = \frac{r - ae^{-i\phi_1}}{1 - rae^{-i\phi_1}} + (a - r^2 a)(ra)^N e^{-iN\phi_1} \\ \times \left(\frac{e^{-i\phi_1}}{1 - rae^{-i\phi_1}} - \frac{e^{-i\phi_0}}{1 - rae^{-i\phi_0}}\right) \end{aligned} \tag{7}$$

where $\frac{r - ae^{-i\phi_1}}{1 - rae^{-i\phi_1}}$ is the static transmission $T(\phi_1)$ when the round-trip phase change is ϕ_1, which can be derived directly from the transfer matrix method. Eq. (7) is exactly the same with $T(\phi_1)$ if $\phi_0 = \phi_1$, which means the ring is in a

steady state. We can make further simplifications to set a relationship between static transmission and transient transmission. In Eq. (7), $(ra)^N e^{-iN\phi_1}$ is a time-dependent term, while $(a-r^2a)(\frac{e^{-i\phi_1}}{1-rae^{-i\phi_1}} - \frac{e^{-i\phi_0}}{1-rae^{-i\phi_0}})$ is constant. One can simplify the time-independent term using the following relationship:

$$T(\phi) = \frac{r-ae^{-i\phi}}{1-rae^{-i\phi}} = r-(a-r^2a)\frac{e^{-i\phi}}{1-rae^{-i\phi}} \tag{8}$$

When $t = N\tau$, we can thus write $T(N\tau)$ as:

$$T(t) = T(\phi_1) + (T(\phi_0) - T(\phi_1))(ra)^{\frac{t}{\tau}} e^{i\frac{\phi_1 t}{\tau}} \tag{9}$$

Eq. (9) sets a relationship between steady-state transmission and transient transmission when the refractive index of the ring is altered. When ϕ of the ring is altered at t > 0, there is still some portion of light which enters the ring at t < 0 traveling in the ring. These lights will "memorize" ϕ of the ring at t < 0, interfere with the output field when coupled to output waveguide, and affect T(t). Before T(t) reaches the steady state, the output field is oscillating described by $e^{-i\phi_1 t/\tau}$ and decaying described by $(ra)^{t/\tau}$. Therefore, under high-speed modulation, it will take some time for the ring to switch from $T(\phi_0)$ to $T(\phi_1)$. The switching time is independent of electrical bandwidth and is described by optical bandwidth in previous works [33].

In silicon photonics, the EO modulation mechanism is the carrier dispersion effect, which means both the refractive index and the loss term is altered during modulation [34]. In this case, we can assume the parameter change can be written as:

$$\phi(t) = \begin{cases} \phi_0 & t \le 0 \\ \phi_1 & t > 0 \end{cases} \quad a(t) = \begin{cases} a_0 & t \le 0 \\ a_1 & t > 0 \end{cases} \tag{10}$$

Then Eq. (3) should be rewritten as [28]:

$$B(t) = rA(t) - \sum_{k=1}^{\infty}\left(\frac{1}{r} - r\right)(r)^k \times \left(\prod_{m=0}^{k-1} a(t-m\tau)\right) e^{-i\sum_{m=0}^{k-1}\phi(t-m\tau)} A(t-k\tau) \tag{11}$$

Using the same approach to deduce Eq. (9), we can also obtain a compact formula to describe the transient transmission:

$$T(t) = T(\phi_1) + (T(\phi_0) - T(\phi_1))(ra_1)^{\frac{t}{\tau}} e^{i\frac{\phi_1 t}{\tau}} \tag{12}$$

Eq. (12) reveals that after switching, the evolving rate of T(t) is determined by parameters of the ring at t > 0, like ϕ_1, a_1. Therefore, the transient transmission of the ring which is switched from ϕ_0 to ϕ_1 is different from that which is switched back from ϕ_1 to ϕ_0.

III. Discussions

A. Modeling Verification

We set the parameters of the ring for simulations based on the state-of-the-art ring to verify Eq. (9) by a reliable commercial simulation software Lumerical Interconnect. The Q factor of the ring with the radius of 5 μm is set as 10^4 in order to obtain an approximated bandwidth of 20 GHz. The extinction ratio (ER) of the ring can reach 20 dB. The loss in the ring is 5 dB/mm.

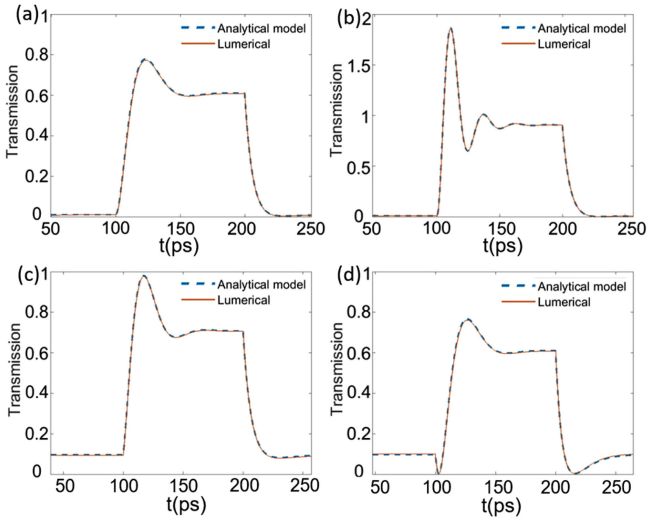

Fig. 2. The comparison of transmission between analytical results calculated by Eq. (9), and simulation results on Lumerical Interconnect under different modulation phases: (a) $[\phi_0, \phi_1] = [0, 0.02]$ (b) $[\phi_0, \phi_1] = [0, 0.05]$ (c) $[\phi_0, \phi_1] = [0.005, 0.025]$ (d) $[\phi_0, \phi_1] = [-0.005, 0.025]$.

A comparison between simulation results on Lumerical interconnect and analytical calculation based on Eq. (9) on Matlab is shown in Fig. 2. The operating speed is 10 Gb/s. The ring is switched from ϕ_0 to ϕ_1 at t = 100 ps, then switched back from ϕ_1 to ϕ_0 at t = 200 ps. Fig. 2 shows the transmission under different phase conditions. We assume the ring has reached a steady state before it is switched. Therefore, Eq. (9) is used twice to describe rise and fall period, respectively. Fig. 2 reveals that Eq. (9) fits well with the simulation results on Lumerical, where the deviation is less than 1.4%.

The oscillating transmission in Fig. 2, known as "overshooting effect" is observed both in experiments and in simulations in previous works [35], [36]. The shape of the overshooting effect depends on $[\phi_0, \phi_1]$ we choose. When ϕ_1 is small, there will be only one peak in the rising period. When ϕ_1 is relatively large, the transmission will oscillate serval times before it reaches a steady state. Fig. 2 reveals the oscillating transmission can be predicted well by Eq. (9). In experiments, ϕ_1 is often limited by modulation amplitude of refractive index. However, to obtain a large modulation depth, ϕ_1 should be large and overshooting effect will be commonly observed when the ring is used as logic gates. When $\phi_0 \neq 0$, the transmission will also oscillate and there will be dips during the rising period and falling period (Fig. 2(d)). More quantitative explanation will be discussed in following sections.

B. Switching Performance

The switching performance of microring modulator is crucial to the accuracy and operating speed of an optical computing system. To enable enough tolerance to noise and other effects in computing, the modulation depth should be high enough to

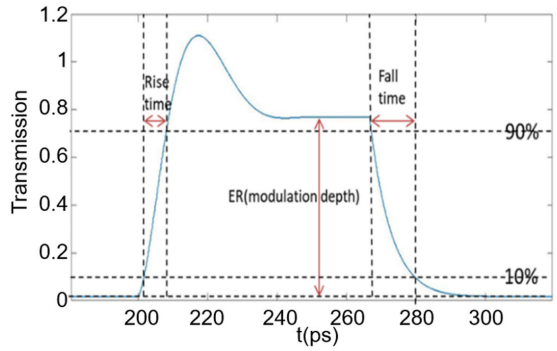

Fig. 3. Modulation depth (ER), rise time, fall time of an optical signal.

differentiate logic 0 and logic 1. The switching time of a single ring will determine the operating speed of the whole system. Even for a single ring, the switching performance will vary according to different phases we choose to represent logic 0 or 1. We will focus on these switching properties of microring resonators under different modulation conditions. It should be noted that only optical dynamics contribute to these switching properties and we do not consider the switching time of phase changes for simplicity. One can use analytical models in [28] to obtain switching performance contributed by both electronic effects and optical dynamics with the help of numerical softwares.

In this paper, we focus on four switching properties: modulation depth, rise time, fall time, and total switching time. Modulation depth is the intensity difference between logic 1 s and logic 0 s. The switching time of microresonators consists of two terms: rise time and fall time. To set an analogy with electronics logic gates [37], we define the rise time of microresonators as the time required for the response to rise from 10% to 90% of modulation depth. Similarly, the fall time is time required for the transmission to change from 90% to 10% of modulation depth. A schematic of these properties in an optical signal is shown in Fig. 3.

Fig. 4 shows the colormaps about the switching performance at different $[\phi_0, \phi_1]$. It contains 1600 modulation conditions when $\phi_0/\phi_1 \in[-0.02\pi, 0.02\pi]$. Four properties including modulation depth, rise time, fall time, and total switching time are illustrated. Such colormap is helpful for us to choose the appropriate bias and amplitude.

Modulation depth can be calculated directly using static model of rings $ER = 20log(T(\phi_1)/T(\phi_0))$. From simulation results, one can find, the ER can be close to 20 dB even when $\Delta\phi$ is small (0.07π) thanks to the high Q factor. When $\Delta\phi$ is fixed, the operating wavelength should be close to resonant wavelength to have a large ER.

In the rising period, the transient transmission is dominated by $(ra)^{\frac{t}{\tau}}e^{-i\frac{\phi_1 t}{\tau}}$ in Eq. (9). The output field intensity is doing a damped oscillation. The damping time constant is $-\frac{\tau}{ln(ra)}$, while the oscillating time constant is $\frac{\tau}{\phi_1}$. When the phase change $\phi_1 > -ln(ra)$, the rise time is dominated by ϕ_1. On the other hand, if *ra* is large, the rise time is dominated by *ra*. From

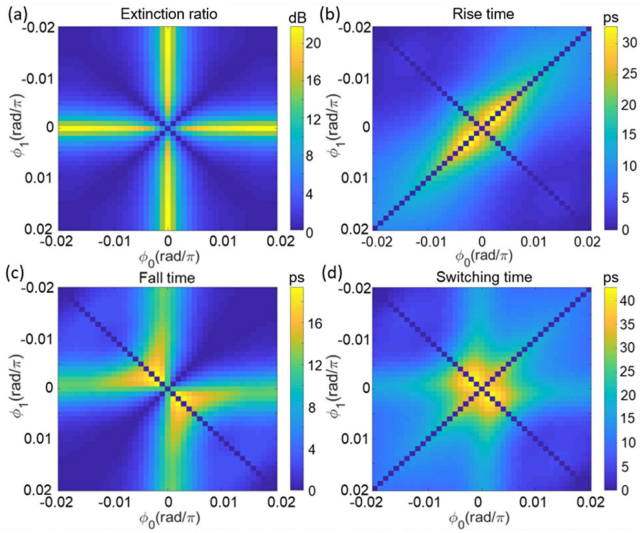

Fig. 4. Switching properties of the ring when $\phi_0/\phi_1 \in[-0.02\pi, 0.02\pi]$. (a) Extinction ratio (b) rise time (c) fall time (d) switching time.

Fig. 4(b) we can learn the larger ϕ_1 is, the shorter rise time will be. However, from Fig. 4(b) we know the transmission will oscillate serval times before reaching a steady state when ϕ_1 is large.

The fall time of the ring is often dominated by the damping time constant $-\frac{\tau}{ln(ra)}$. In order to obtain a deep modulation depth, the ring should be on resonance when transmitting logic 0, which means $\phi_1 = 2m\pi$, *m* is an integer. Because $t/\tau = N$ is also an integer, $e^{-i\frac{\phi_0 t}{\tau}} = 1$, only the damping time constant $-\frac{\tau}{ln(ra)}$ will dominate fall time. In Fig. 4(c), it can be shown that when $\phi_0 = 0$, the fall time is constant. In order to have a large modulation depth, $\phi_1 > -ln(ra)$, therefore the rise time is often shorter than the fall time.

C. Cascading Logic

In an optical computing architecture, multiple rings/disks modulators will be put in series to realize some complex logic functions, which will bring some cascading issues. Unlike MOSFET-based hardware, where repeaters and latches are available to prevent electrical signals from degradation during propagation, optical logic signals inevitably decay and deteriorate when passing through optical devices and waveguide. Therefore, the noise and imperfectness of previous optical logic signals will also propagate to next bit computing. When errors and imperfectness accumulate, the logic of the output signal will be deteriorated.

Here we investigate the cascading logic of microdisk modulators, the Lumerical compact model of which is provided by AIM Photonics PDK and parameters of the model are obtained from experiments[38], [39]. Though the mechanism of microdisks and microrings are similar, microdisks are more welcomed than microrings modulators in optical computing because of smaller footprint and lower power consumption [40].

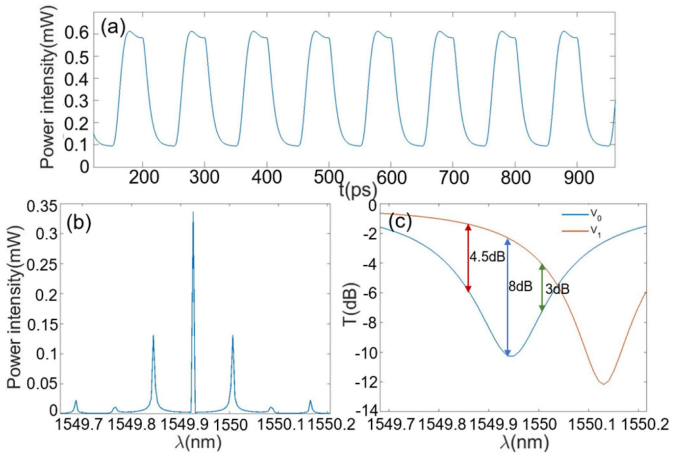

Fig. 5. Output power intensity of the disk when it is switched between V_0 and V_1 periodically. The input power intensity is 1 mW. The modulation speed is 20 Gb/s. The output optical power intensity is shown in (a) time domain, (b) wavelength domain. (c) Modulation depth of different wavelengths. Modulation depths of operating wavelength (1549.94 nm) and wavelengths corresponding to first harmonics sidebands (1549.84 nm, 1550.04 nm) are shown.

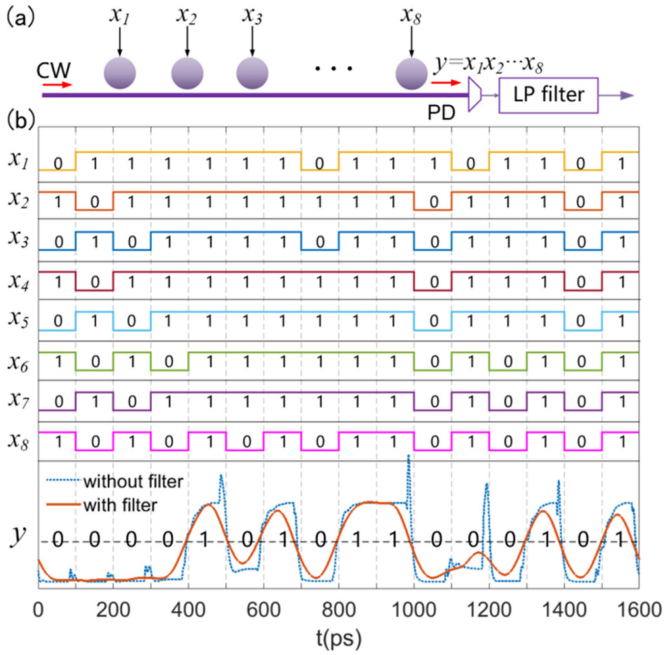

Fig. 6. (a) The schematics of 8-bit AND gate, output signal $y = x_1x_2 \ldots x_7x_8$. (b) Logic inputs and output waveforms. Operation speed is 10 Gbits/s. The output result not using low pass filter is shown in blue dashed line. The output result using low pass filter to filter the signal is shown in red solid line. Reference line showing the logic threshold level is drawn by a black dashed line.

The first factor that will make logic signals imperfect is overshooting effect. As we can infer from Fig. 3, the transmission after a continuous wave (CW) light propagates the first ring is logically correct. However, the propagating light signal is not a perfect square wave because of switching time and overshooting effect. Because of the overshooting effect, the transient transmission *T(t)* can exceed the static transmission $T(\phi_1)$ in the rising period. What is worse, from Fig. 3, we can infer that the rise time is much shorter than the fall time when the ER is high. Therefore, the previous peaks caused by the overshooting effect cannot be cut off if the microresonator is switching from 1 to 0. When multiple resonators are cascaded in series, and all of them are switching from 0 to 1, the overshooting effect will be serious.

Another factor that will make the logic signal nonideal is the wavelength-dependent transmission of the rings or "sideband effect". After an ideal CW light with wavelength λ_0 propagates a ring modulated by digital signals, the modulated light with output field intensity *B(t)* will have multiple sidebands in the frequency domain, which can be described by:

$$\mathcal{F}(e^{(-j2\pi f_0 t)}B(t)) = \mathcal{B}(f - f_0) \tag{13}$$

where $\mathcal{F}$ is the Fourier transform operator, $\mathcal{B}(f)$ is *B(t)* in frequency domain, $f_0 = \frac{2\pi c}{\lambda_0}$. In the wavelength domain, Eq. (13) means the modulated light $e^{(-j2\pi f_0 t)}B(t)$ has multiple wavelengths. We define these wavelengths in addition to the operating wavelength λ_0 as sidebands. To each wavelength, $[\phi_0, \phi_1]$ will be different from each other. As we can see from Fig. 4(a), the ER of a microresonator is highly dependent on $[\phi_0, \phi_1]$ with a quality factor of around 5000. As shown in Fig. 5, output power intensities of the microdisk modulator in time domain and wavelength domain are shown. The disk is modulated periodically at 20 Gb/s. From Fig. 5(c), one can find ERs of sidebands are less than that of operating wavelength. Sideband effect will reduce the intensity differences between logic 0 s and logic 1 s, and the quality of optical waveform as well. The transmission of a microdisk array will be worse than a simple multiplication of constituent microdisks' transmissions owing to sideband effect. Sideband effect cannot be evaluated with the dynamic model of a single modulator in previous works [28]. Instead, one needs to expand modulated light in the wavelength domain, then use Eq. (12) to calculate the transmission of each wavelength with corresponding $[\phi_0, \phi_1]$, and finally, summarize the output contributed by all sidebands as well as the operating wavelength to obtain the actual transmission of microresonator modulator arrays.

When the number of microresonators is relatively large, the logic result will be deteriorated because of these two factors. Shown in Fig. 6, eight disks are cascaded in an optical path. The output logic is $Y = X_1X_2X_3 \ldots X_7X_8$. One can find that when Y is switching from 0 to 1 or from 1 to 0, the rising period and the falling period are not smooth. From 1100 ps to 1200 ps, as can be seen in the Fig. 6(b), a peak whose intensity is higher than that of logic 1 signals appears while the current logic of this bit should be 0. As a result, the output waveform cannot convey logic correctly, while the waveform quality will be worse at higher bitrate. In comparison, a single microdisk modulator is capable of transmitting 25 Gbs NRZ data [39], meaning sideband effect and overshooting effect will limit the bandwidth of optical computing module consisting of multiple cascaded microresonator modulators even when the EO time constant is smaller than one bit period.

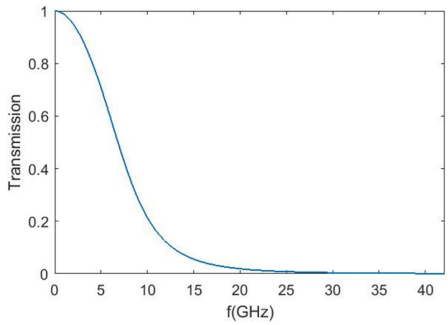

Fig. 7. Transmission of electrical low pass (LP) filter used in this article. It is a 4th order Bessel filter. The bandwidth of the filter is 5 GHz.

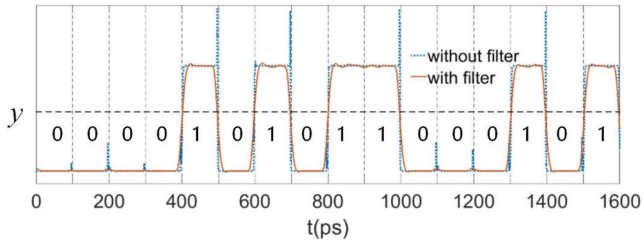

Fig. 8. The schematics of 8-bit AND gate, output signal $y = x_1x_2 \ldots x_7x_8$. Q-factor of each microresonator is 413.2. Logic inputs and operating speed are the same with that in Fig. 6. The output result not using low pass filter is shown in blue dashed line. The output result using low pass filter to filter the signal is shown in red solid line. Reference line showing the logic threshold level is drawn by a black dashed line. The bandwidth of the LP filter is 20 GHz.

Here we suggest adding a low-pass (LP) electrical filter at the output in order to filter the peaks and dips caused by overshooting effect and sideband effect. The transmission of the filter is shown in Fig. 7. From Eq. (9), the time period of the overshooting effect is much shorter than the time period of digital signals. Therefore, peaks caused by overshooting effect can be eliminated by adding a low-pass filter at the end of the output after (optical-electrical) OE conversion. Further, high-frequency sidebands can also be cut off by low-pass filters. The only negative effect is that the rise time and the fall time of logic output will increase. In Fig. 6(b), we perform an electrical LP Bessel filter after the photodetector. One can find all 16 desired logic states have been realized.

Choosing an appropriate time to sample the logic output is an alternative to enable correctness of cascading logic. We can delay the time to read the logic and add some triggers after OE conversion. One can obtain the eye diagram of the computing module and the best sampling time can be set where the eye opening is the biggest. In this way, only the regions where logics are correct will be read so that logic outputs can be sent to the next module without distortion or errors.

On the other hand, we conclude microresonators modulators with low Q factors ($\sim$30) are suitable for functioning as EO logic gates, which can be found in previous works [41]. Shown in Fig. 8, the simulated output waveform is logically correct without adding a low-pass filter under same logic inputs and operating speed while Q-factor of each microresonator modulator is reduced to 413.2. It is known that Q factor is defined as [42]:

$$Q = \frac{\pi n_g L \sqrt{ra}}{\lambda_{res}(1-ra)} \tag{14}$$

Eq. (14) reveals when sizes, propagating modes, and resonant wavelengths of microresonators remain the same, *ra* would be much smaller in rings with lower Q factor. Consequently, smaller *ra* will lead to shorter fall time. According to Eq. (9), smaller *ra* also means the overshooting effect will be reduced because the transient term is decaying fast. The transmission of low Q-factor microresonators is also less sensitive to wavelength deviations. Therefore, both the overshooting effect and sideband effect will be reduced by using low Q-factor microresonator modulators in optical computing systems.

IV. Conclusion

We have presented a compact model to describe the switching dynamics of microresonator modulators. The model is based on the time-dependent transfer matrix and deduced by multiple-round loop approaches. A compact analytical solution of the step response of ring resonator modulator is presented. The solution sets a relationship between static transmission and dynamic transmission. Our model is verified subsequently by comparison with Lumerical Interconnect simulation results.

We focus on switching properties of rings. Serval important switching properties, including switching time, rise time, fall time and extinction ratio are investigated under different modulation phase biases and amplitudes. Factors dominating these behaviors are investigated and explained quantitatively.

Finally, we investigate computing systems where multiple microresonators are linearly cascaded in an optical path. We believe the overshooting effect and sideband effect of microresonators are two major effects deteriorating the output logic. We simulate the performance of microdisk modulators provided by current foundries. We suggest putting one low-pass electrical filter after OE conversion can significantly reduce the cascading problem and improve the waveform quality. We also believe a microresonator modulator with a low Q factor will also reduce cascading problems.

Overall, our compact dynamic model of microresonator modulators reveal their switching properties when they function as EO logic gates. Ways to reduce cascading problems of rings enable design of complicate computing architectures where multiple rings are cascaded.

References

[1] J. Hardy and J. Shamir, "Optics inspired logic architecture," *Opt. Exp.*, vol. 15, no. 1, p. 150, Jan. 2007.

[2] C. Qiu, X. Ye, R. Soref, L. Yang, and Q. Xu, "Demonstration of reconfigurable electro-optical logic with silicon photonic integrated circuits," *Opt. Lett.*, vol. 37, no. 19, p. 3942, Oct. 2012.

[3] Z. Ying *et al.*, "Automated logic synthesis for electro-optic logic-based integrated optical computing," *Opt. Exp.*, vol. 26, no. 21, p. 28002, Oct. 2018.

[4] Z. Zhao *et al.*, "Optical computing on silicon-on-insulator-based photonic integrated circuits," in *Proc. IEEE 12th Int. Conf. ASIC (ASICON)*, 2017, pp. 472–475.

[5] D. R. Solli and B. Jalali, "Analog optical computing," *Nat. Photon.*, vol. 9, no. 11, pp. 704–706, Nov. 2015.

[6] A. Shinya *et al.*, "Low-latency optical parallel adder based on a binary decision diagram with wavelength division multiplexing scheme," in *Proc. Opt. Data Sci.: Trends Shaping Future Photon.*, 2018, vol. 10551, p. 5.

[7] C. A. Thraskias *et al.*, "Survey of photonic and plasmonic interconnect technologies for Intra-Datacenter and High-Performance computing communications," *IEEE Commun. Surv. Tuts.*, vol. 20, no. 4, pp. 2758–2783, Fourth quarter 2018.

[8] D. A. B. Miller, "Optical interconnects to electronic chips," *Appl. Opt.*, vol. 49, no. 25, p. F59, Sep. 2010.

[9] C. Sun *et al.*, "Single-chip microprocessor that communicates directly using light," *Nature*, vol. 528, no. 7583, pp. 534–538, Dec. 2015.

[10] A. H. Atabaki *et al.*, "Integrating photonics with silicon nanoelectronics for the next generation of systems on a chip," *Nature*, vol. 556, no. 7701, pp. 349–354, Apr. 2018.

[11] Q. Xu, B. Schmidt, S. Pradhan, and M. Lipson, "Micrometre-scale silicon electro-optic modulator," *Nature*, vol. 435, no. 7040, pp. 325–327, May 2005.

[12] M. Pantouvaki *et al.*, "56 Gb/s ring modulator on a 300 mm silicon photonics platform," in *Proc. Eur. Conf. Opt. Commun.*, 2015, pp. 1–3.

[13] M. R. Watts, D. C. Trotter, R. W. Young, and A. L. Lentine, "Ultralow power silicon microdisk modulators and switches," in *Proc. 5th IEEE Int. Conf. Group IV Photon.*, 2008, pp. 4–6.

[14] T. Baba *et al.*, "50-Gb/s ring-resonator-based silicon modulator," *Opt. Exp.*, vol. 21, no. 10, p. 11869, May 2013.

[15] E. Timurdogan *et al.*, "An ultralow power athermal silicon modulator," *Nat. Commun.*, vol. 5, no. 1, p. 4008, Dec. 2014.

[16] Z. Ying *et al.*, "Electro-optic ripple-carry adder in integrated silicon photonics for optical computing," *IEEE J. Sel. Top. Quantum Electron.*, vol. 24, no. 6, Nov./Dec. 2018, Art. no. 7600310.

[17] Y. Tian, L. Zhang, R. Ji, L. Yang, and Q. Xu, "Demonstration of a directed optical encoder using microring-resonator-based optical switches," *Opt. Lett.*, vol. 36, no. 19, p. 3795, Oct. 2011.

[18] L. Zhang *et al.*, "Electro-optic directed logic circuit based on microring resonators for XOR/XNOR operations," *Opt. Exp.*, vol. 20, no. 11, p. 11605, May 2012.

[19] Y. Tian, L. Zhang, Q. Xu, and L. Yang, "XOR/XNOR directed logic circuit based on coupled-resonator-induced transparency," *Laser Photon. Rev.*, vol. 7, no. 1, pp. 109–113, Jan. 2013.

[20] Z. Ying *et al.*, "Silicon microdisk-based full adders for optical computing," *Opt. Lett.*, vol. 43, no. 5, p. 983, Mar. 2018.

[21] L. Zhang *et al.*, "Demonstration of directed XOR/XNOR logic gates using two cascaded microring resonators," *Opt. Lett.*, vol. 35, no. 10, p. 1620, May 2010.

[22] D. Gostimirovic and W. N. Ye, "Ultracompact CMOS-compatible optical logic using carrier depletion in microdisk resonators," *Sci. Rep.*, vol. 7, no. 1, p. 12603, Dec. 2017.

[23] Y. Tian *et al.*, "Experimental demonstration of a reconfigurable electro-optic directed logic circuit using cascaded carrier-injection micro-ring resonators," *Sci. Rep.*, vol. 7, no. 1, p. 6410, Dec. 2017.

[24] Z. Liu *et al.*, "On-chip optical parity checker using silicon photonic integrated circuits," *Nanophotonics*, vol. 7, no. 12, pp. 1939–1948, 2018.

[25] Q. Xu and R. Soref, "Reconfigurable optical directed-logic circuits using microresonator-based optical switches," vol. 19, no. 6, pp. 5244–5259, 2011.

[26] W. D. Sacher and J. K. S. Poon, "Dynamics of microring resonator modulators," *Opt. Exp.*, vol. 16, no. 20, p. 15741, Sep. 2008.

[27] H. Yu *et al.*, "Trade-off between optical modulation amplitude and modulation bandwidth of silicon micro-ring modulators," *Opt. Exp.*, vol. 22, no. 12, p. 15178, Jun. 2014.

[28] R. Dube-Demers *et al.*, "Analytical modeling of silicon microring and microdisk modulators with electrical and optical dynamics," *J. Lightw. Technol.* vol. 33, no. 20, pp. 4240–4252, Oct. 2015.

[29] M. Minkov, Y. Shi, and S. Fan, "Exact solution to the steady-state dynamics of a periodically modulated resonator," *APL Photon.*, vol. 2, no. 7, p. 076101, Jul. 2017.

[30] K.-P. Ho and J. M. Kahn, "Optical frequency comb generator using phase modulation in amplified circulating loop," *IEEE Photon. Technol. Lett.*, vol. 5, no. 6, pp. 721–725, Jun. 1993.

[31] R. A. Cohen, O. Amrani, and S. Ruschin, "Linearized electro-optic racetrack modulator based on double injection method in silicon," *Opt. Exp.*, vol. 23, no. 3, p. 2252, Feb. 2015.

[32] S. Feng, T. Lei, H. Chen, H. Cai, X. Luo, and A. W. Poon, "Silicon photonics: From a microresonator perspective," *Laser Photon. Rev.*, vol. 6, no. 2, pp. 145–177, Apr. 2012.

[33] O. Dubray *et al.*, "Electro-optical ring modulator : An ultracompact model for the comparison and optimization," *IEEE J. Sel. Top. Quantum Electron.*, vol. 22, no. 6, Nov./Dec. 2016, Art. no. 3300110.

[34] R. Soref and B. Bennett, "Electrooptical effects in silicon," *IEEE J. Quantum Electron.*, vol. QE-23, no. 1, pp. 123–129, Jan. 1987.

[35] C.-M. Chang, G. de Valicourt, P. Dong, and S. Chandrasekhar, "Differential microring modulators for intensity and phase modulation: Theory and experiments," *J. Lightw. Technol.*, vol. 35, no. 15, pp. 3116–3124, Aug. 2017.

[36] Q. Xu, B. Schmidt, J. Shakya, and M. Lipson, "Cascaded silicon micro-ring modulators for WDM optical interconnection," *Opt. Exp.*, vol. 14, no. 20, p. 9431, Oct. 2006.

[37] J. Rabaey, A. Chandrakasan, and B. Nikolic, *Digital Integrated Circuits.* Upper Saddle River, NJ, USA: Prentice-Hall, 2002.

[38] A. Photonics, "American institute of manufacturing integrated photonics," 2016. [Online]. Available: http://www.aimphotonics.com/pdk/. [Accessed: 16-Mar-2019].

[39] E. Timurdogan *et al.*, "APSUNY Process Design Kit (PDKv3.0): O, C and L band silicon photonics component libraries on 300 mm wafers," in *Proc. 2019 Opt. Fiber Commun. Conf. Exhib.,* p. Tu2A.1, 2019.

[40] Z. Ying *et al.*, "Comparison of microrings and microdisks for high-speed optical modulation in silicon photonics," *Appl. Phys. Lett.*, vol. 112, no. 11, p. 111108, Mar. 2018.

[41] C. Haffner *et al.*, "Low-loss plasmon-assisted electro-optic modulator," *Nature*, vol. 556, no. 7702, pp. 483–486, Apr. 2018.

[42] W. Bogaerts *et al.*, "Silicon microring resonators," *Laser Photon. Rev.*, vol. 6, no. 1, pp. 47–73, Jan. 2012.

Chenghao Feng received the B.S degree in physics from Nanjing University, Nanjing, China, in 2018. He is currently working toward the Ph.D. degree in electrical and computer engineering, University of Texas at Austin, Austin, TX, USA. His research interests include silicon photonics devices and system design for optical computing and interconnect in integrated photonics.

Zhoufeng Ying received the B.E. and M.E. degrees in optical engineering from Nanjing University, Nanjing, China, in 2014 and 2016, respectively. He is currently working toward the Ph.D degree in electrical and computer engineering, University of Texas at Austin, Austin, TX, USA. His research interests include optical computing and interconnect in integrated photonics.

Zheng Zhao received the B.S. degree in automation from Tongji University, Shanghai, China, in 2012 and the M.S degree in electrical and computer engineering from Shanghai Jiao Tong University, Shanghai, China, in 2015. She is currently working toward the Ph.D. degree in electrical and computer engineering, University of Texas at Austin, Austin, TX, USA under the supervision of Prof. David Z. Pan. Her research interests include optical computing/interconnect and logic synthesis.

Rohan Mital received the B.E. degree in electronics and communication engineering from the Indian Institute of Information Technology Guwahati, Guwahati, India, in 2017. He is currently working toward the Ph.D. degree in electrical and computer engineering, University of Texas at Austin, Austin, TX, USA. His research interests include optical computing and interconnect in integrated photonics.

David Z. Pan (Fellow, IEEE) received the B.S. degree from Peking University, Beijing, China and the M.S. and Ph.D. degrees from the University of California, Los Angeles (UCLA), Los Angeles, CA, USA. From 2000 to 2003, he was a Research Staff Member with IBM T. J. Watson Research Center. He is currently the Engineering Foundation Professor with the Department of Electrical and Computer Engineering, the University of Texas at Austin, Austin, TX, USA. His research interests include cross-layer IC design for manufacturability, reliability, security, physical design, analog design automation, and CAD for emerging technologies. He has authored more than 300 technical papers and is the holder of eight U.S. patents. He has graduated more than 20 Ph.D. students who are now holding key academic and industry positions. He has served as a Senior Associate Editor for *ACM Transactions on Design Automation of Electronic Systems*, an Associate Editor for the IEEE TRANSACTIONS ON COMPUTER AIDED DESIGN OF INTEGRATED CIRCUITS AND SYSTEMS, the IEEE TRANSACTIONS ON VERY LARGE SCALE INTEGRATION SYSTEMS, IEEE TRANSACTIONS ON CIRCUITS AND SYSTEMS PART I, the IEEE TRANSACTIONS ON CIRCUITS AND SYSTEMS PART II, IEEE DESIGN & TEST, SCIENCE CHINA INFORMATION SCIENCES, *Journal of Computer Science and Technology*, IEEE CAS Society Newsletter, etc. He was in the Executive and Program Committees of many major conferences, including DAC, ICCAD, ASPDAC, and ISPD. He is the ASPDAC 2017 Program Chair, ICCAD 2018 Program Chair, DAC 2014 Tutorial Chair, and ISPD 2008 General Chair. He was the recipient of a number of awards for his research contributions, including the SRC 2013 Technical Excellence Award, DAC Top ten Author in Fifth Decade, DAC Prolific Author Award, ASP-DAC Frequently Cited Author Award, 14 Best Paper Awards at premier venues (HOST 2017, SPIE 2016, ISPD 2014, ICCAD 2013, ASPDAC 2012, ISPD 2011, IBM Research 2010 Pat Goldberg Memorial Best Paper Award, ASPDAC 2010, DATE 2009, ICICDT 2009, SRC Techcon in 1998, 2007, 2012 and 2015) plus 11 additional Best Paper Award nominations at DAC/ICCAD/ASPDAC/ISPD, Communications of the ACM Research Highlights (2014), ACM/SIGDA Outstanding New Faculty Award (2005), NSF CAREER Award (2007), SRC Inventor Recognition Award three times, IBM Faculty Award four times, UCLA Engineering Distinguished Young Alumnus Award (2009), UT Austin RAISE Faculty Excellence Award (2014), and many international CAD contest awards, among others. He is a Fellow of SPIE.

Ray T. Chen (Fellow, IEEE) received the B.S degree in physics from the National Tsing Hua University in Taiwan, Hsinchu, Taiwan, in 1980, the M.S. degree in physics and the Ph.D. degree in electrical engineering both from the University of California, Oakland, CA, USA, in 1983 and 1988, respectively. He is the Keys and Joan Curry/Cullen Trust Endowed Chair with The University of Texas at Austin, Austin, TX, USA. He is the Director of the Nanophotonics and Optical Interconnects Research Lab, Microelectronics Research Center. He is also the Director of the AFOSR MURI-Center for Silicon Nanomembrane involving faculty from Stanford, UIUC, Rutgers, and UT Austin. He joined UT Austin in 1992 to start the optical interconnect research program. From 1988 to 1992, he worked as a Research Scientist, Manager, and the Director with the Department of Electro-Optic Engineering, Physical Optics Corporation in Torrance, California. He was the CTO, Founder, and Chairman of the Board of Radiant Research, Inc. from 2000 to 2001, where he raised 18 million dollars A-Round funding to commercialize polymer-based photonic devices involving over twenty patents, which were acquired by Finisar in 2002, a publicly traded company in the Silicon Valley (NASDAQ:FNSR). He also serves as the founder and Chairman of the Board of Omega Optics Inc. since its initiation in 2001. Omega Optics has received more than five million dollars in research funding. His research work has been awarded over 135 research grants and contracts from such sponsors as Army, Navy, Air Force, DARPA, MDA, NSA, NSF, DOE, EPA, NIST, NIH, NASA, the State of Texas, and private industry. The research topics are focused on four main subjects: (1) Nano-photonic passive and active devices for bio- and EM-wave sensing and interconnect applications, (2) Thin film guided-wave optical interconnection and packaging for 2D and 3D laser beam routing and steering, (3) True time delay (TTD) wide band phased array antenna (PAA), and (4). 3D printed micro-electronics and photonics. Experiences garnered through these programs are pivotal elements for his research and further commercialization. Dr. Chen's group at UT Austin has reported its research findings in more than 900 published papers, including more than 100 invited papers. He holds more than 60 patents. He has chaired or been a Program-Committee Member for more than 120 domestic and international conferences organized by IEEE, SPIE (The International Society of Optical Engineering), OSA, and PSC. He was an Editor, Co-Editor or Coauthor for over twenty-five books. He has also served as a consultant for various federal agencies and private companies and delivered numerous invited/plenary talks to professional societies. He is a Fellow of OSA and SPIE. He was the recipient of the 1987 UC Regent's Dissertation Fellowship and the 1999 UT Engineering Foundation Faculty Award, for his contributions in research, teaching and services. He received the Honorary Citizenship Award in 2003 from the Austin City Council for his contribution in community service. He was also the recipient of the 2008 IEEE Teaching Award, and the 2010 IEEE HKN Loudest Professor Award. 2013 NASA Certified Technical Achievement Award for contribution on moon surveillance conformable phased array antenna. During his undergraduate years at the National Tsing Hua University, he led the 1979 university debate team to the Championship of the Taiwan College-Cup Debate Contest. Dr. Chen has supervised and graduated 50 Ph.D. students from his research group with UT Austin. Many of them are currently professors in the major research universities in USA and abroad.